Figures and figure supplements

Downregulation of Dickkopf-3, a Wnt antagonist elevated in Alzheimer's disease, restores synapse integrity and memory in a disease mouse model

Nuria Martin Flores and Marina Podpolny *et al*.

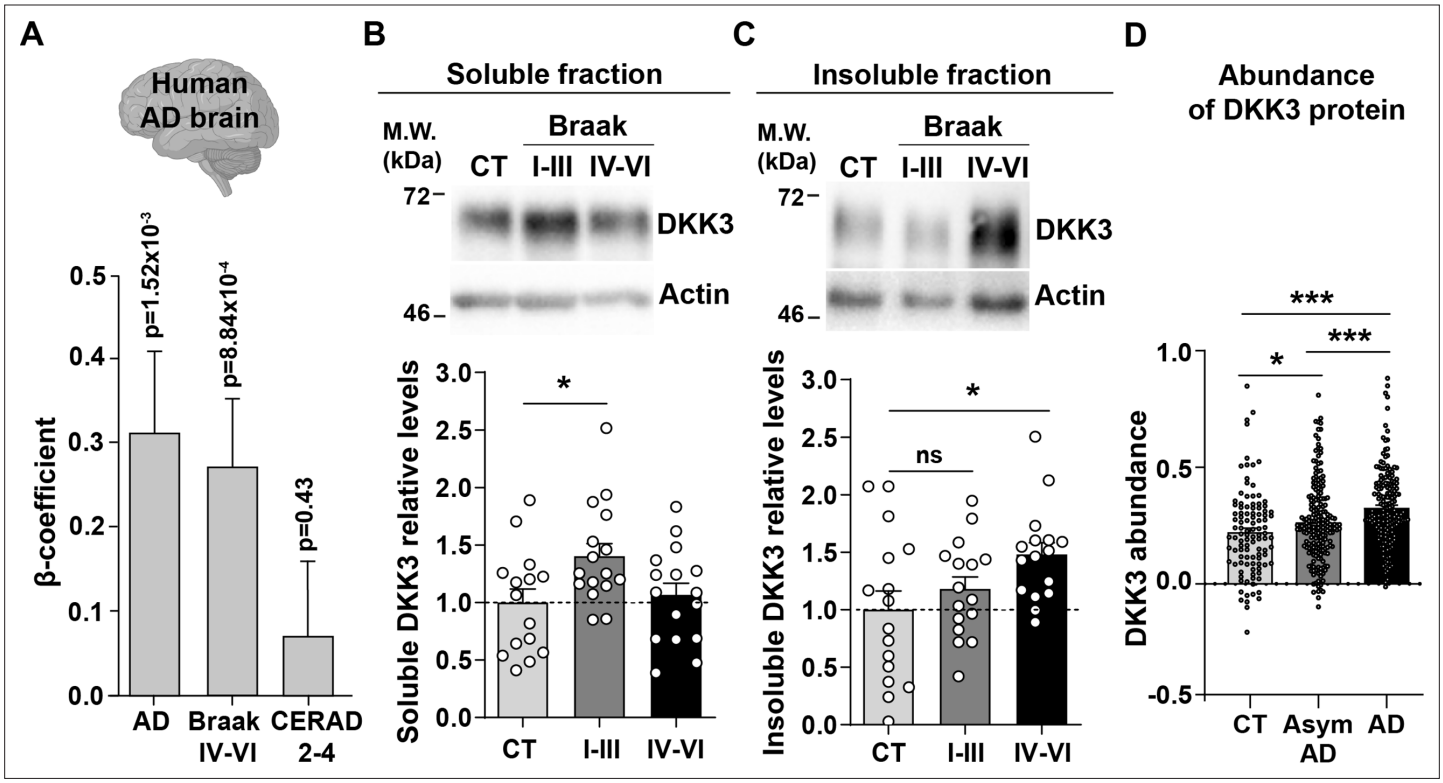

Figure 1. DKK3 mRNA and protein levels are increased in the human AD brain. (**A**) Temporal cortex RNAseq dataset logistic regression shows that *DKK3* mRNA levels are increased in AD cases relative to controls. Ordinal regression shows that *DKK3* is differentially expressed for Braak scores IV-VI but not for CERAD scores 2–4. (**B, C**) Representative immunoblots of DKK3 and loading control actin in (**B**) soluble and (**C**) insoluble protein fractions from the hippocampus of control (CT; n=15–16), Braak stages I-III (n=16), and Braak stage IV-VI (n=16) individuals (One-Way ANOVA test followed by Tukey's multiple comparisons). See also ***Supplementary file 1***. (**D**) Abundance of DKK3 protein in dorsolateral prefrontal cortex from control CT, n=106, asymptomatic (Asym) AD (n=200), and AD (n=182) individuals was evaluated using a tandem mass tag mass spectrometry (TMT-MS) proteomic dataset study (***Johnson et al., 2022***) (ANOVA with two-sided Holm correction, AD vs CT p-value = 0.00000168, Asym AD vs. CT p-value = 0.042492481, AD vs. Asym AD = 0.000402907).

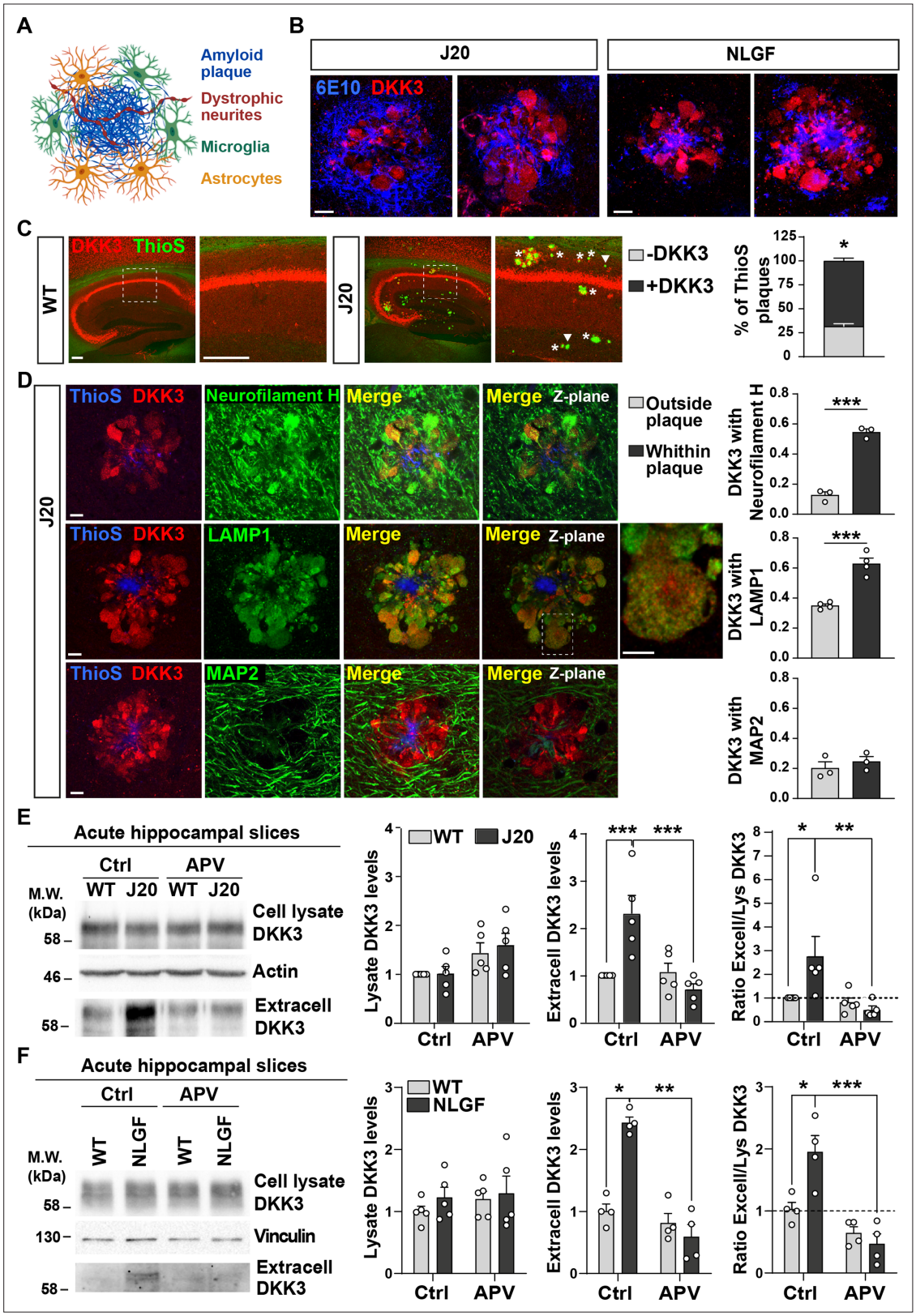

Figure 2. DKK3 localizes to dystrophic neurites around Aβ plaques, and DKK3 extracellular levels are increased in the brain of AD mouse models. (**A**) Diagram of the components of an Aβ plaque (blue), astrocytes (orange), microglia (green), and dystrophic neurites (red). (**B**) Confocal images of DKK3 protein (red) and amyloid plaques stained with the 6E10 antibody (blue) in the hippocampus of 18-month-old J20 and 8 months NLGF mice. Scale bar = 10 μm. (**C**) Confocal images of DKK3 (red) and Aβ plaques labeled by Thioflavin S (ThioS; green) in the hippocampus of 18-month-old WT

Figure 2 continued on next page

Figure 2 continued

and J20 mice. ThioS +plaques not containing DKK3 (- DKK3; arrowheads), ThioS +plaques containing DKK3 (+DKK3; asterisks). Scale bar = 150 μm and 100 μm in zoom-in pictures. Graph depicts quantification of the percentage of ThioS +plaques containing or not DKK3 (Student's T-test, n=3 animals per genotype). (**D**) Z-stack confocal images show that DKK3 (red) accumulates at Aβ plaques (ThioS; blue) and colocalizes with atrophic axons (Neurofilament-H; green and LAMP1; green) but not with dendrites (MAP2; green). XY views of one plane are shown in the last panel. For LAMP1, a zoom-in picture showing colocalization between DKK3 and LAMP1 puncta is shown. Scale bar = 6 μm. Graphs show Pearson's correlation coefficient between DKK3 and Neurofilament-H, LAMP1, or MAP2, n=3–4 animals. (**E, F**) Immunoblot images show DKK3 levels in the cell lysate and secreted fraction of acute hippocampal slices of (**E**) 3–4 month-old WT and J20 mice or (**F**) 2–3 months old WT and NLGF mice. Slices were incubated with vehicle (Ctrl) or APV for 3 hr. Actin or Vinculin was used as a loading control in the homogenate. Graphs show densitometric quantifications of lysate and extracellular (extracell) DKK3 levels relative to control and the ratio of extracellular/lysate DKK3 levels (Two-Way ANOVA followed by Tukey's post-hoc test; n=4–5 animals).

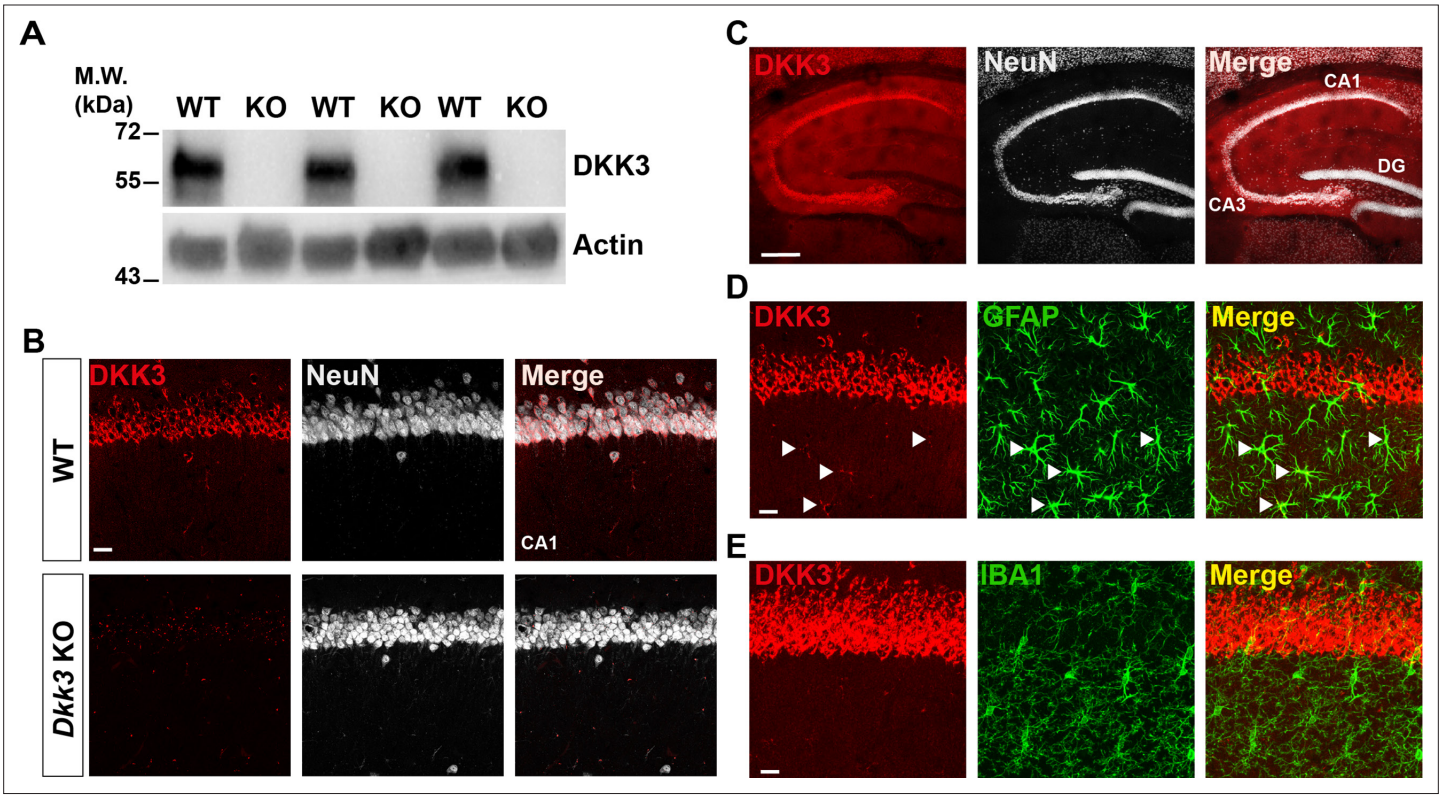

Figure 2—figure supplement 1. DKK3 is present in principal neurons of the mouse hippocampus. (**A**) Immunoblotting images show the presence or absence of DKK3 protein in hippocampal homogenates of WT and *Dkk3*$^{-/-}$*ApoE*$^{-/-}$ (KO) mice demonstrate the specificity of the antibody against DKK3. Actin was used a loading control. (**B**) Confocal images show DKK3 protein in the CA1 region of the hippocampus in WT mice but absent in the *Dkk3*$^{-/-}$*ApoE*$^{-/-}$ (KO) mice. Scale bar = 25 µm. (**C**) Confocal images of DKK3 (red) and neuronal marker NeuN (grey) demonstrate that DKK3 colocalizes with principal neurons but not with granular neurons in the hippocampus. Scale bar = 250 µm. (**D**) Confocal images of DKK3 (red) and the astrocyte marker GFAP (green). Arrowheads indicate some astrocytes expressing low levels of DKK3. Scale bar = 25 µm. (**E**) Confocal images of DKK3 (red) and microglial marker IBA1 (green). Scale bar = 25 µm.

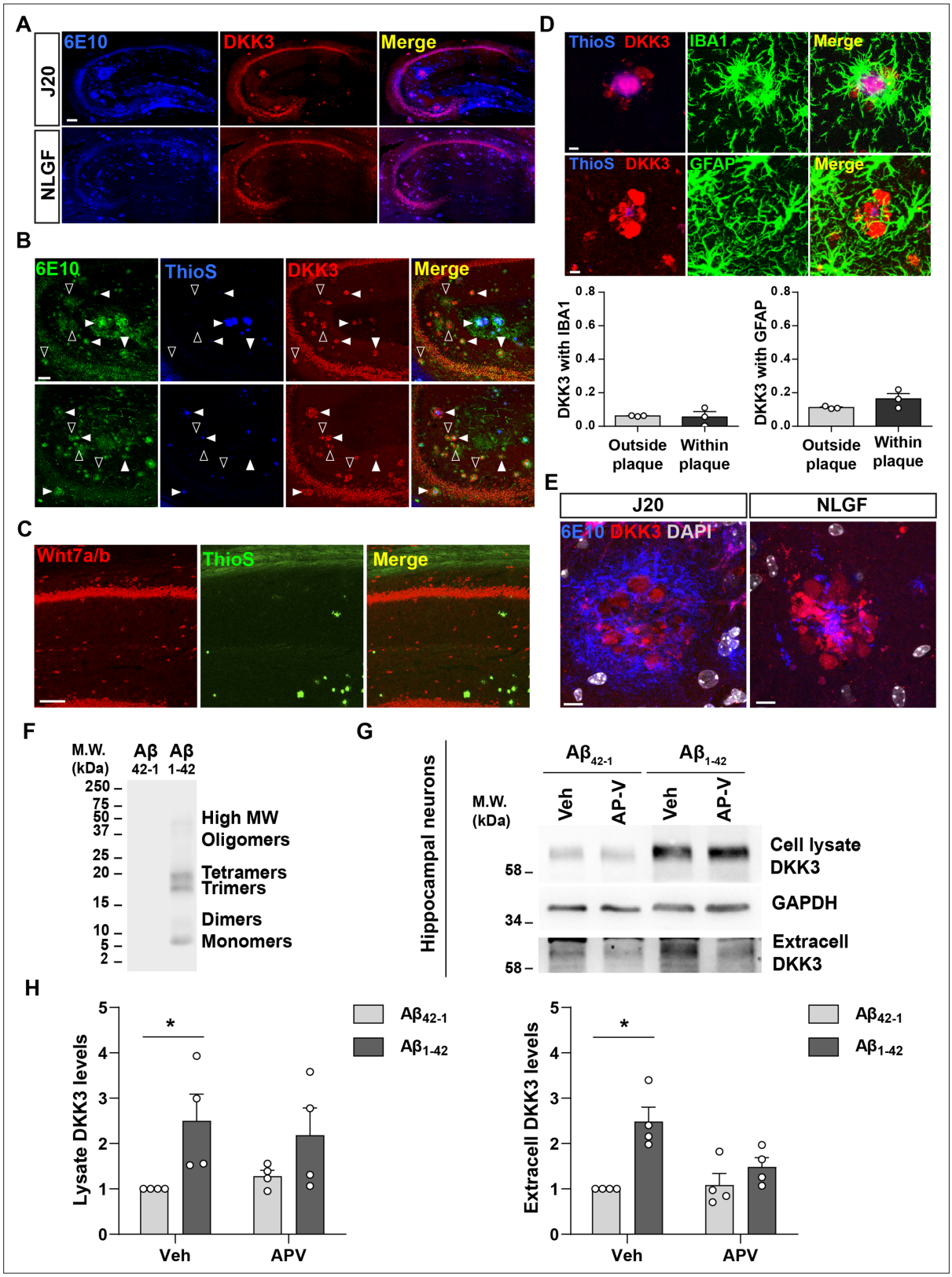

Figure 2—figure supplement 2. DKK3 accumulates in Aβ plaques in the hippocampus of J20 and NLGF mice and DKK3 levels are increased by Aβ. (**A**) Confocal images of Aβ plaques (6E10, blue) and DKK3 (red) in the hippocampus of 12-month-old J20 and 8-month-old NLGF mice. Scale bar = 140 µm. (**B**) Confocal images show that DKK3 (red) accumulates in Aβ plaques (6E10, green) with or without a dense-core (ThioS, blue) in 18-month-old J20 hippocampi. Empty arrowheads indicate diffuse plaques (6E10 positive, ThioS negative) containing DKK3. White arrowheads point to dense-core

Figure 2—figure supplement 2 continued on next page

Figure 2—figure supplement 2 continued

plaques (positive for 6E10 and ThioS) containing DKK3. Scale bar = 58 μm. (**C**) Confocal images of Wnt7a/b (red) and Aβ plaques stained by Thioflavin S (ThioS, green) in the CA1 region of 18-month-old J20 mice. Scale bar = 100 μm. (**D**) Z-stack confocal images showing DKK3 (red) in Aβ plaques (ThioS, blue) and microglia (IBA1, green) or astrocytes (GFAP, green). Scale bar = 6 μm. Graphs show the Pearson's coefficient quantification showing the degree of colocalization between DKK3 and IBA1 or GFAP, n=3 animals. (**E**) Confocal images of Aβ plaques (6E10, blue), DKK3 (red), and DAPI staining of nuclei (grey) in the hippocampus of 12-month-old J20 and 8-month-old NLGF mice. Scale bar = 8 μm. (**F**) Preparation of oligomers of $A\beta_{1\text{-}42}$ (Aβo). Representative immunoblots of 6E10 for $A\beta_{42\text{-}1}$ (reverse peptide control) and $A\beta_{1\text{-}42}$. (**G**) Representative immunoblot image shows DKK3 levels in the lysate and in extracellular media of cultured hippocampal neurons treated with reverse Aβ peptide ($A\beta_{42\text{-}1}$) or Aβo ($A\beta_{1\text{-}42}$) and vehicle (Veh) or APV. GAPDH was used as a loading control in cell lysates. (**H**) Graphs show densiometric quantifications of lysate and extracellular (extracell) DKK3 levels relative to control (Kruskal-Wallis followed by Dunn's post-hoc test; n=4 independent experiments).

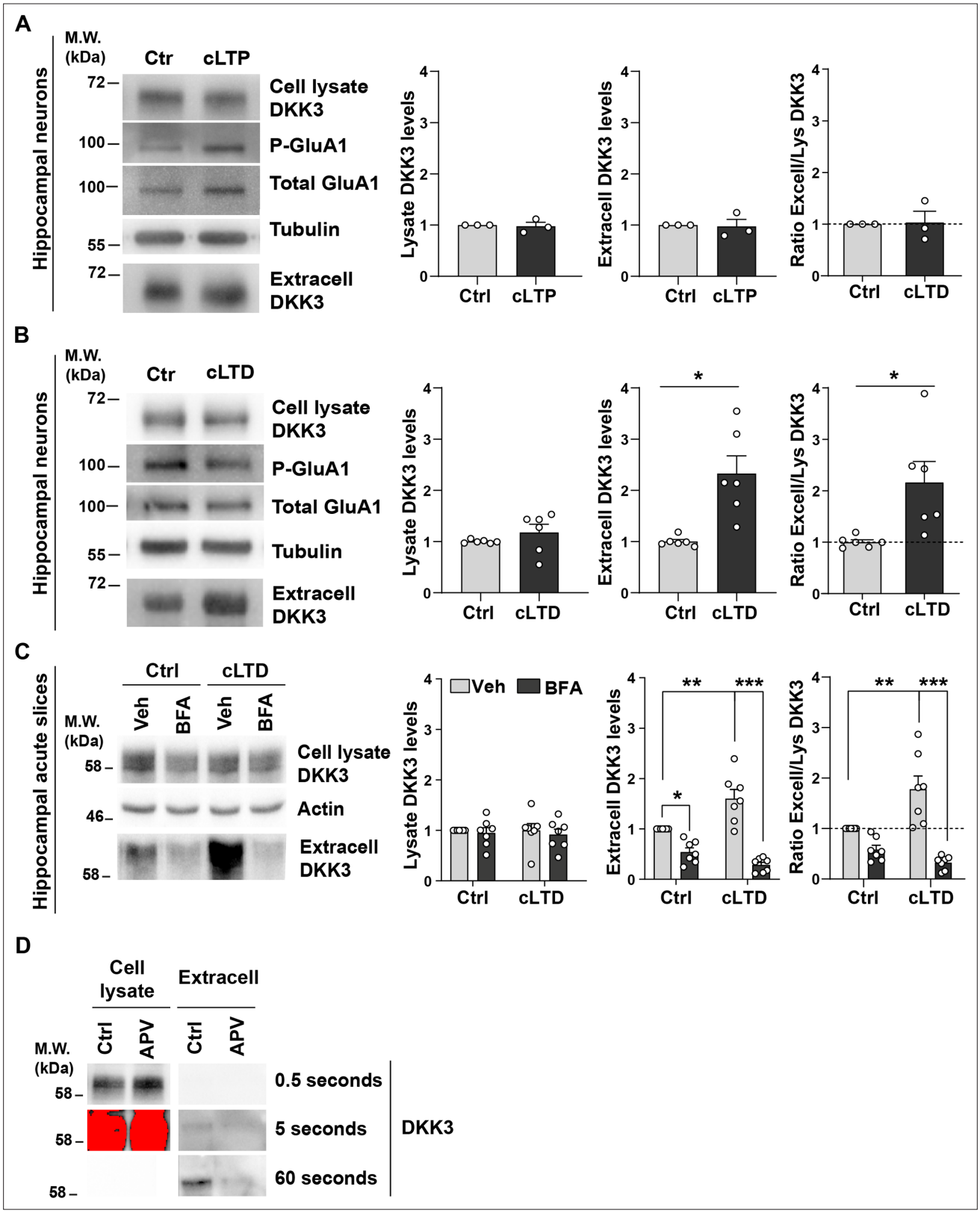

Figure 2—figure supplement 3. cLTD, but not cLTP, increases the levels of extracellular DKK3. (**A, B**) Hippocampal neurons were subjected to (**A**) chemical LTP (cLTP) or (**B**) chemical LTD (cLTD). DKK3 levels were analyzed in the supernatant (extracell) and cell lysates by western blot. Phospho-GluA1 Ser845 was used as a readout of LTP and LTD induction, and tubulin as a loading control for the cell lysate. Graphs show the levels of DKK3 relative to control and the ratio of extracellular/lysate DKK3 levels (Mann-Whitney Test, n=3 independent cultures for cLTP and Student's T-test, n=6

Figure 2—figure supplement 3 continued on next page

Figure 2—figure supplement 3 continued

independent cultures for cLTD). (**C**) Representative immunoblots show DKK3 levels in the cell lysate and extracellular (extracell) fraction of acute WT hippocampal slices treated with vehicle (Ctrl) or NMDA (cLTD) and/or Brefeldin A (BFA) for 60 min. Actin was used as a loading control in homogenates. Graphs show densiometric quantifications of DKK3 relative to the control condition and the ratio of extracellular/lysate DKK3 levels (Kruskal-Wallis followed by Dunn's multiple comparisons; n=5 animals). (**D**) Immunoblot showing DKK3 is less abundant in the extracellular fraction when compared to the cell lysate fraction. Representatives immunoblot of J20 brain slices treated with control or APV for 3 hr. Time exposure for obtaining DKK3 chemiluminescent images is indicated.

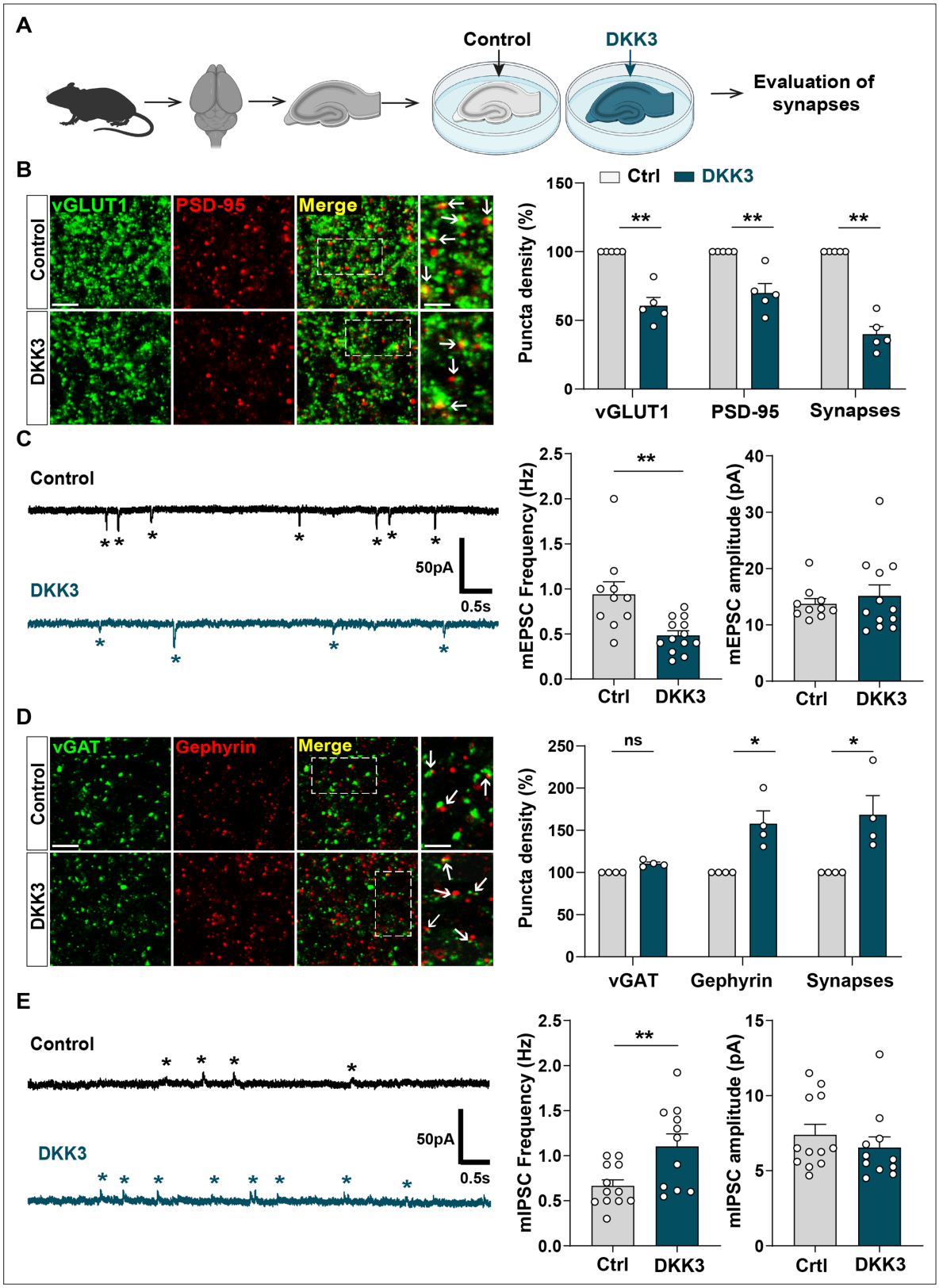

Figure 3. Gain-of-function of DKK3 leads to opposing effects on the number of excitatory and inhibitory synapses in the hippocampus. (**A**) Diagram depicting the treatment of hippocampal brain slices obtained from 3-month-old adult WT mice with vehicle (Ctrl) or recombinant DKK3 protein. Synapses were evaluated by confocal microscopy and electrophysiological recordings. (**B**) Confocal images of the CA3 SR region labeled with the presynaptic excitatory marker vGLUT1 (green) and the postsynaptic marker PSD-95 (red). Arrows indicate excitatory synapses as colocalized pre- and

Figure 3 continued on next page

Figure 3 continued

postsynaptic puncta. Scale bar = 5 μm and 2.5 μm in zoomed-in pictures. Quantification is shown on the right-hand side (Mann-Whitney test, n=5 animals per condition). (**C**) Representative mEPSC traces recorded at –60 mV from CA3 cells. Stars indicate mEPSC events. Quantification of mEPSC frequency and amplitude is shown on the right-hand side (Mann-Whitney test, n=10–13 cells from five animals). (**D**) Confocal images of the CA3 SR region labeled with the presynaptic inhibitory marker vGAT (green) and the postsynaptic marker gephyrin (red). Arrows indicate inhibitory synapses as colocalized pre- and postsynaptic puncta. Scale bar = 5 μm and 2.5 μm in zoomed-in pictures. Quantification is shown on the right-hand side (Mann-Whitney test, n=4 animals per condition). (**E**) Representative mIPSC traces recorded at 0 mV from CA3 cells. Stars indicate mIPSC events. Quantification of mIPSC frequency and amplitude is shown on the right-hand side (Student's T-test for mIPSC frequency and Mann-Whitney test for mIPSC amplitude, n=11–12 cells from five to seven animals).

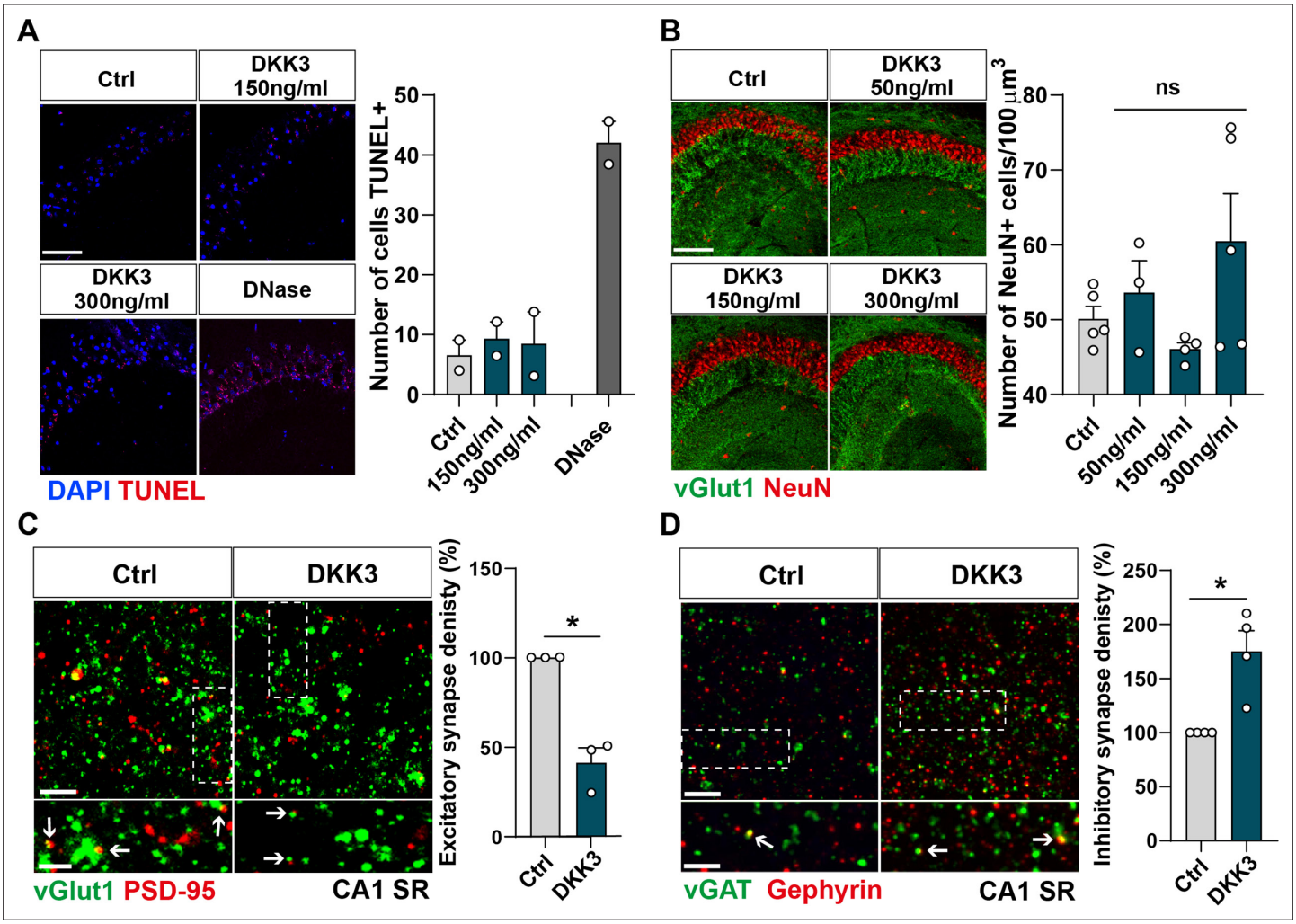

Figure 3—figure supplement 1. DKK3 triggers changes in excitatory and inhibitory synapses in the absence of cell death. (**A**) Confocal images of the TUNEL assay (red) in the hippocampus CA3 area (DAPI in blue). Graph shows the number of cells positive for TUNEL. Scale bar = 20 µm (n=2 animals). (**B**) Confocal images show the impact of different DKK3 concentrations on cell number (NeuN in red) and vGLUT1 (green) in the hippocampus CA3 area. Graph shows the number of NeuN + cells per 100 µm^3. Scale bar = 150 µm (One-way ANOVA followed by Tukey's post-hoc test, ns, n=2 animals, 2–3 brain slices per animal). (**C**) Confocal images from hippocampal CA1 SR show the effect of DKK3 on excitatory synapses (colocalized vGLUT1 puncta in green and PSD-95 puncta in red). Arrows indicate excitatory synapses. Scale bar = 5 µm and 2.5 µm in zoomed-in pictures. Quantification is shown on the right-hand side (Mann-Whitney test, n=3 animals). (**D**) Confocal images from hippocampal CA1 SR show the effect of DKK3 on inhibitory synapses (colocalized vGAT puncta in green and gephyrin puncta in red). Arrows point to inhibitory synapses. Scale bar = 5 µm and 2.5 µm in zoomed-in pictures. Quantification is shown on the right-hand side (Mann-Whitney test, n=4 animals).

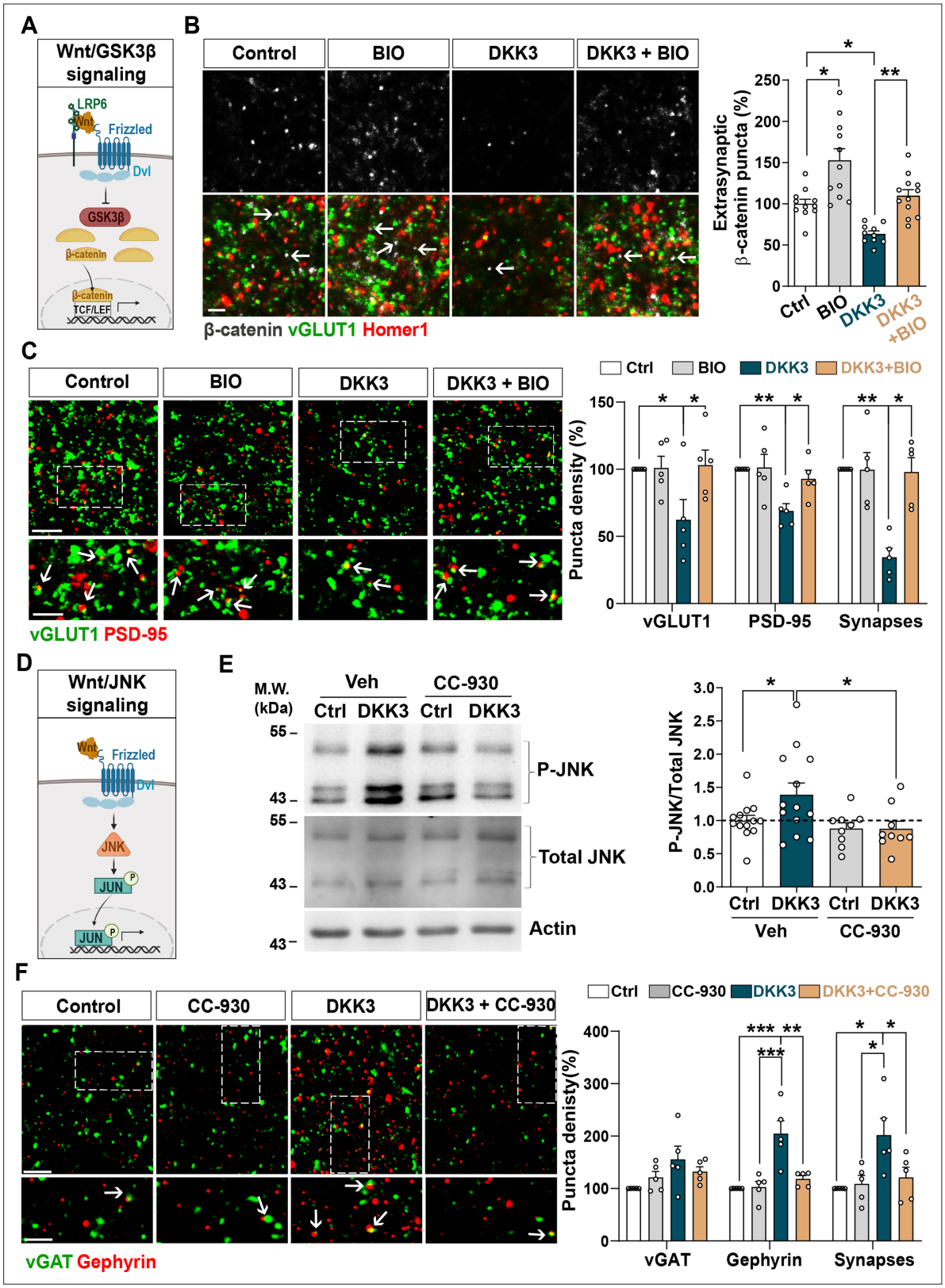

Figure 4. DKK3 regulates excitatory and inhibitory synapse number through the Wnt/GSK3β and Wnt/JNK pathways respectively. (**A**) Diagram of the canonical Wnt pathway through inhibition of GSK3β (Wnt/GSK3β pathway), resulting in elevation of β-catenin and transcriptional activation via TCF/LEF. (**B**) Confocal images show excitatory synapses, visualized by colocalization of vGLUT1 (green) and Homer1 (red), as well as β-catenin puncta (grey) in the CA3 SR after treatment with vehicle (Ctrl) or DKK3 in the absence or presence of BIO. Arrows indicate extra-synaptic β-catenin puncta. Scale bar =

Figure 4 continued on next page

Figure 4 continued

5 µm. Quantification of extrasynaptic β-catenin puncta density as a percentage of control is shown on the right-hand side (Two-Way ANOVA followed by Tukey's multiple comparisons, n=2–3 brain slices/animal from five animals). (**C**) Confocal images show excitatory synapses (co-localized vGLUT1 puncta in green and PSD-95 puncta in red) in the CA3 SR after treatment with vehicle (Ctrl) or DKK3 in the absence or presence of BIO. Scale bar = 5 µm and 2.5 µm. Graph shows the quantification of puncta density of pre- and postsynaptic markers and excitatory synapses as a percentage of control (Kruskal-Wallis followed by Dunn's multiple comparisons, n=5 animals). (**D**) Diagram of the Wnt pathway through activation of JNK (Wnt/JNK pathway), resulting in increased levels of phospho-JNK and transcriptional changes. (**E**) Representative immunoblots of phospho-JNK Thr183/Tyr185 (P-JNK) and total JNK of brain slices treated with DKK3 and/or the JNK inhibitor CC-930. Actin was used as a loading control. Graph shows densitometric quantification of P-JNK vs. total JNK relative to the control condition (Kruskal-Wallis followed by Dunn's multiple comparisons, n=2 brain slices/animal from four to five animals). (**F**) Confocal images showing inhibitory synapses defined by the colocalization of vGAT (green) and gephyrin (red) puncta in the CA3 SR after treatment with vehicle (Ctrl) or DKK3 in the absence or presence of CC-930. Scale bar = 5 µm and 2.5 µm. Graph shows the quantification of puncta density of pre and postsynaptic markers and inhibitory synapses as a percentage of control (Kruskal-Wallis followed by Dunn's multiple comparisons, n=5 animals).

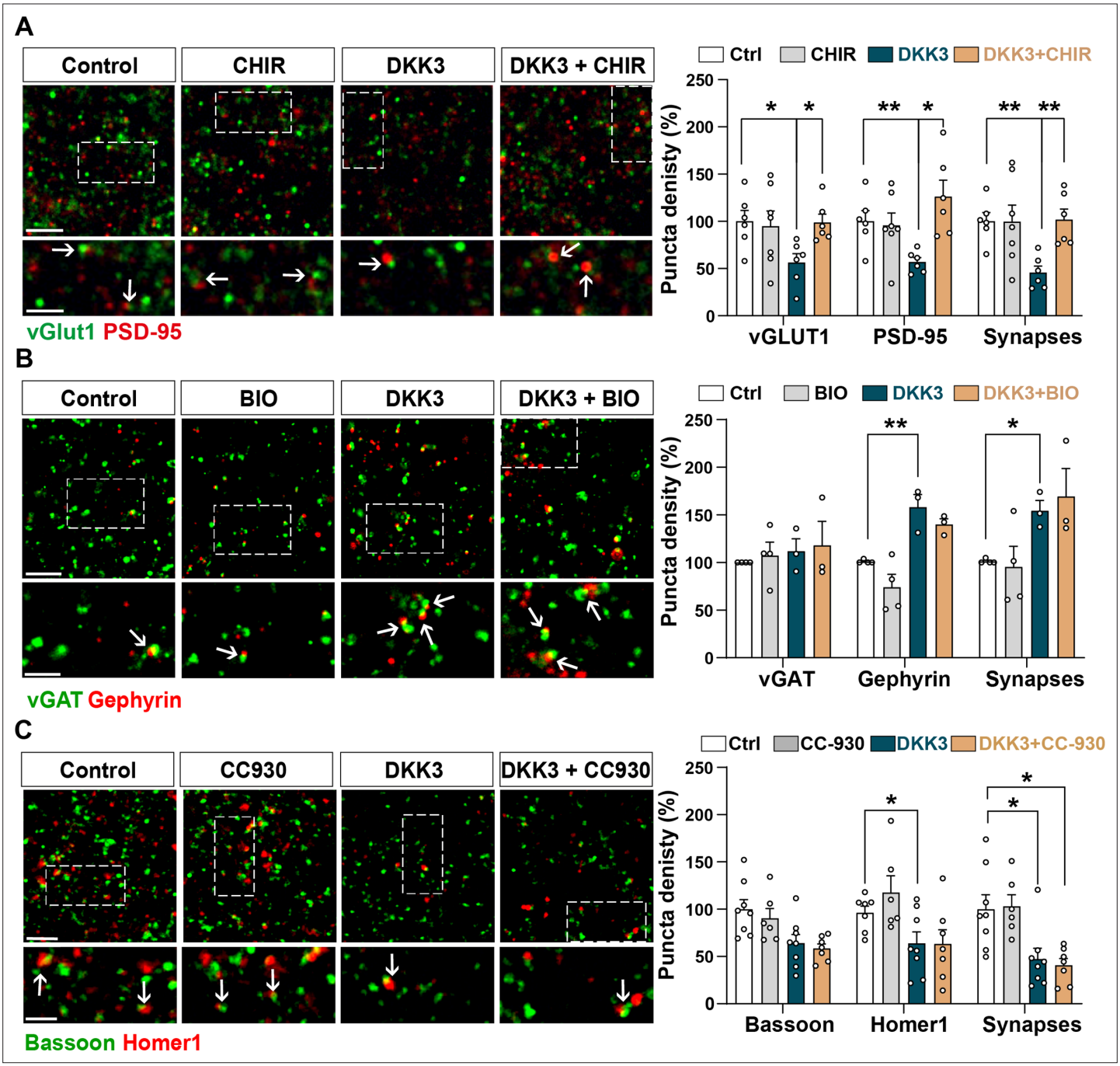

Figure 4—figure supplement 1. Activation of the Wnt/GSK3β pathway blocks DKK3-induced excitatory synapse loss whereas inhibition of the Wnt/JNK pathway blocks the effect of DKK3 on inhibitory synapses. (**A**) Confocal images show excitatory synapses (co-localized vGLUT1 in green and PSD-95 in red) in the CA3 SR after treatment with vehicle (Ctrl) or DKK3 in the absence or presence of CHIR99021 (CHIR) for 4 hr. Scale bar = 5 µm and 2.5 µm Graph shows the quantification of puncta density for pre and postsynaptic markers as well as excitatory synapse number as a percentage of control (Kruskal-Wallis followed by Dunn's multiple comparisons, n=2–3 brain slices from three animals). (**B**) Confocal images showing inhibitory synapses defined by the colocalization of vGAT (green) and Gephyrin (red) in the CA3 SR after treatment with vehicle (Ctrl) or DKK3 in the absence or presence of BIO. Scale bar = 5 µm and 2.5 µm. Graph shows the quantification of puncta density of pre and postsynaptic markers as well as inhibitory synapse number as a percentage of control (Kruskal-Wallis followed by Dunn's multiple comparisons, n=3–4 animals). (**C**) Confocal images showing excitatory synapses (colocalized Bassoon in green and Homer1 in red) in the CA3 SR after vehicle (Ctrl) or DKK3 treatment in the absence or presence of CC-930. Scale bar = 5 µm and 2.5 µm. Graph shows the quantification of pre and postsynaptic markers as well as excitatory synapse number as a percentage of control (Two-Way ANOVA followed by Tukey's multiple comparisons, n=2–3 brain slices from three animals).

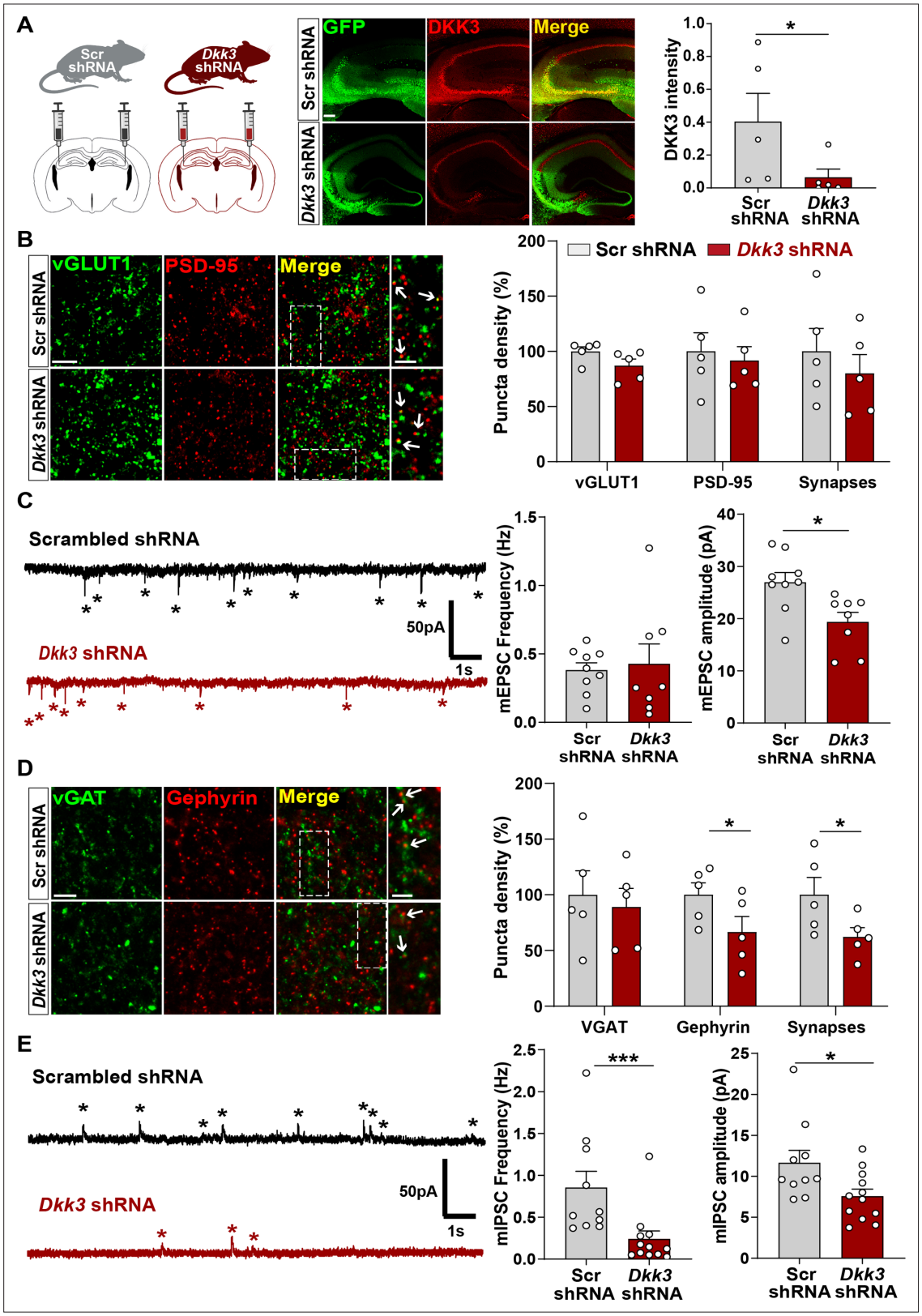

Figure 5. In vivo loss-of-function of DKK3 decreases inhibitory synapses but does not affect excitatory synapses in the wild-type hippocampus. (**A**) Diagram showing the experimental design. Three-month-old WT mice were injected with AAV9 scrambled (Scr) or *Dkk3* shRNA in the CA3 region. Confocal images showing GFP (green) and DKK3 (red) in Scr- and *Dkk3*-shRNA injected hippocampus. Scale bar = 145 µm. Graph shows quantification of DKK3 intensity in the area injected with the viruses. (**B**) Confocal images from CA3 SR show excitatory synapses (colocalized vGLUT1 puncta in green

Figure 5 continued on next page

Figure 5 continued

and PSD-95 puncta in red). Arrows indicate excitatory synapses. Scale bar = 5 μm and 2.5 μm in zoomed-in images. Quantification is shown on the right-hand side (Student's T-test, n=5 animals per condition). (**C**) Representative mEPSC traces recorded at –60 mV from CA3 cells. Stars indicate mEPSC events. Quantification of mEPSC frequency and amplitude is shown on the right-hand side (Student's T-test, n=8–9 cells from four animals). (**D**) Confocal images from CA3 SR show inhibitory synapses (colocalized vGAT in green and gephyrin in red). Arrows point to inhibitory synapses. Scale bar = 5 μm and 2.5 μm in zoomed-in pictures. Quantification is shown on the right-hand side (Student's T-test, n=5 animals). (**E**) Representative mIPSC traces recorded at 0 mV from CA3 cells. Stars indicate mIPSC events. Quantification of mIPSC frequency and amplitude is shown on the right-hand side (Mann-Whitney test, n=10–12 cells from six animals).

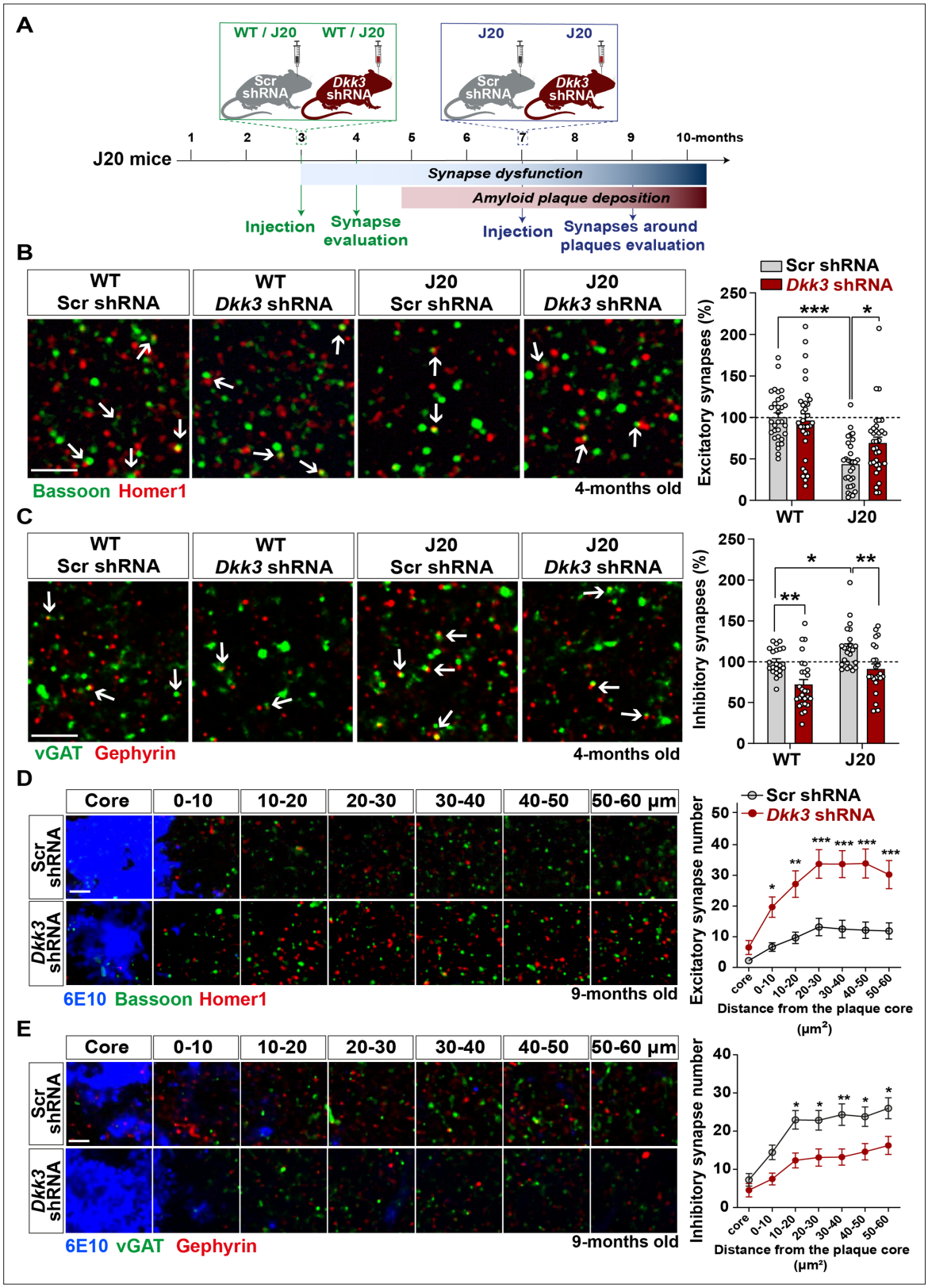

Figure 6. In vivo loss-of-function of DKK3 ameliorates synaptic changes in the hippocampus of J20 mice before and after Aβ plaque formation. (**A**) Diagram depicting the experimental design. In green, 3-month-old WT and J20 mice were injected bilaterally with AAV9-Scr shRNA or AAV9-*Dkk3* shRNA in the CA3 region. The density of synapses was evaluated at 4-month-old before plaque deposition starts. In blue, 7-month-old J20 mice were injected bilaterally with AAV9-Scr shRNA or AAV9-*Dkk3* shRNA in the CA3 region. The density of synapses around plaques was evaluated at 9-month-

Figure 6 continued on next page

Figure 6 continued

old. (**B, C**) Representative confocal images from the CA3 SR region of 4-month-old WT and J20 mice. Images show (**B**) excitatory synapses (Bassoon in green and Homer1 in red) and (**C**) inhibitory synapses (vGAT in green and Gephyrin in red). Arrows point to synapses. Scale bar = 2.5 μm. Quantification of synapse number as a percentage relative to WT-Scr shRNA animals is shown on the right-hand side (Two-Way ANOVA followed by Tukey's post-hoc test, n=9–11 animals per condition and 2–3 brain slices per animal). (**D, E**) Representative confocal images from the CA3 SR region of 9-month-old J20 mice. Images show an Aβ plaque (6E10; blue) and (**D**) excitatory synapses or (**C**) inhibitory synapses at different distances relative to the core of the plaque. Scale bar = 2.5 μm. Graphs show synapse number per 200 μm^3 at each distance (Two-Way ANOVA followed by Tukey's post-hoc test, n=6–7 animals per condition and 2–3 brain slices per animal).

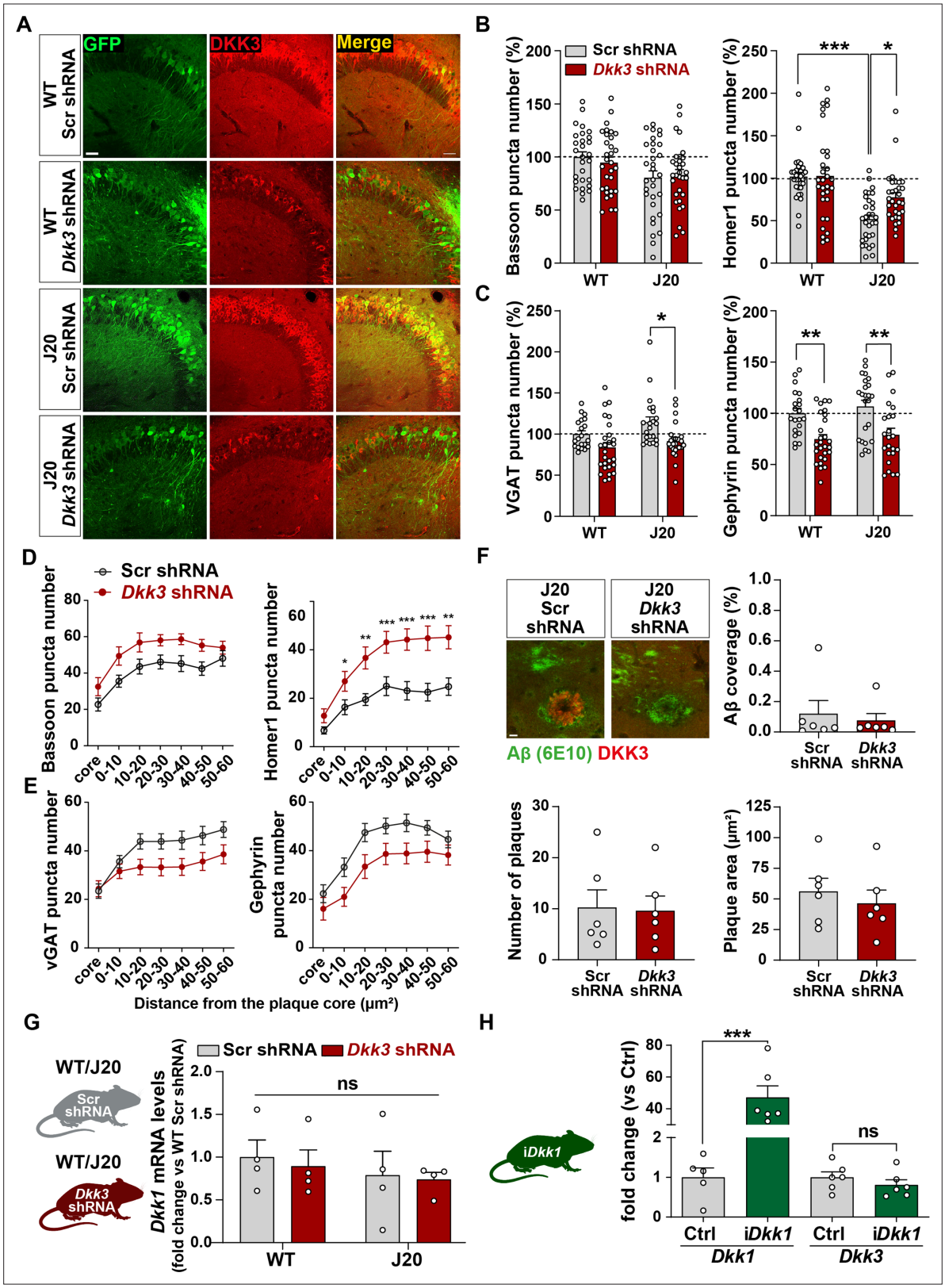

Figure 6—figure supplement 1. In vivo DKK3 loss-of-function affects pre- and postsynaptic markers but does not affect Aβ plaque pathology or *Dkk1* expression in the mouse hippocampus. (**A**) Confocal images of the CA3 area of the hippocampus show that endogenous DKK3 is downregulated in the hippocampus of wildtype and J20 injected with *Dkk3* shRNA AAV9 virus. Scale bar = 38 µm. (**B, C**) Graphs show (**B**) excitatory (Bassoon and Homer1) and (**C**) inhibitory (vGAT and Gephyrin) puncta density as a percentage relative to WT Scr shRNA group in 4 months old WT and J20 mice (Two-Way

Figure 6—figure supplement 1 continued on next page

Figure 6—figure supplement 1 continued

ANOVA followed by Tukey's post-hoc test, n=9–11 animals per condition and 3 brain slices per animal). (**D, E**) Graphs show (**D**) excitatory (Bassoon and Homer1) and (**E**) inhibitory (vGAT and Gephyrin) puncta density at each distance from the core plaque as density per 200 μm^3 in 9 months old J20 mice (Two-Way ANOVA followed by Tukey's post-hoc test. n=7–8 animals per condition and 3 brain slices per animal). (**F**) DKK3 downregulation does not affect plaque load in the hippocampus. Confocal images of Aβ (6E10 in green) and DKK3 (red) in the CA3 SR of 9 months old J20 mice. Scale bar = 10 µm. Graphs show the quantification of Aβ coverage, plaque number and plaque area in the CA3 (Student's T-test, ns, n=6 per condition). (**G**) DKK3 downregulation does not affect *Dkk1* expression in the hippocampus. *Dkk1* expression was evaluated in the hippocampus of 4-month-old WT and J20 mice injected with Scr or *Dkk3* shRNA. Graph shows *Dkk1* mRNA levels normalized to the control group (Kruskal-Wallis followed by Dunn's multiple comparisons, ns, n=4 animals per condition). (**H**) Increased expression of *Dkk1* does not affect *Dkk3* mRNA levels. *Dkk3* expression was examined in the hippocampus of *iDkk1* mice compared to control mice after induction of *Dkk1* for 14 days. Graph shows *Dkk1* and *Dkk3* mRNA levels normalized to the control group (Student's T-test, n=5–6 animals per condition).

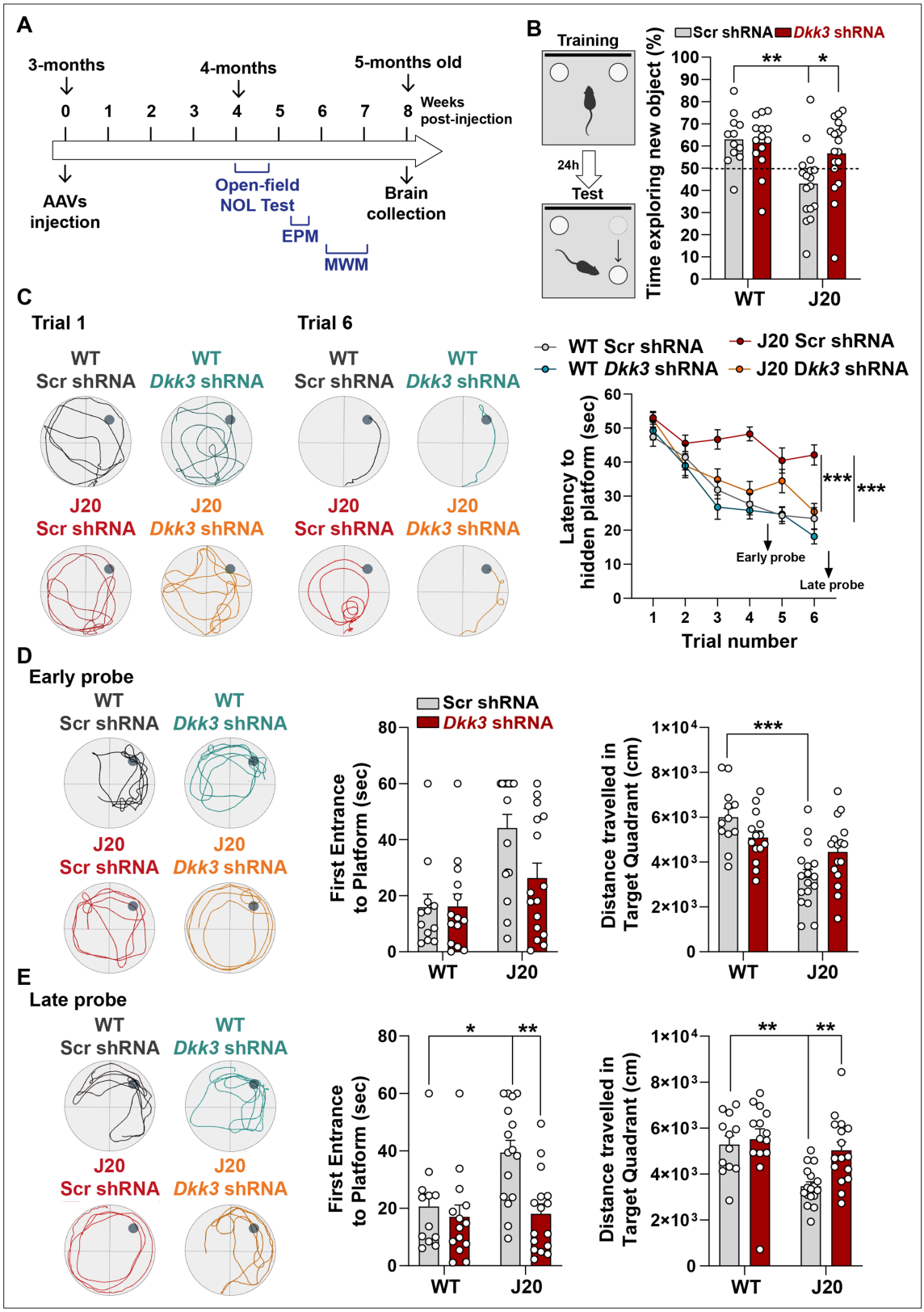

Figure 7. In vivo loss-of-function of DKK3 improves spatial memory in J20 mice. (**A**) Diagram depicting that 3-month-old WT and J20 mice were injected bilaterally with AAV9-Scr shRNA or AAV9-*Dkk3* shRNA in the CA3 area of the hippocampus. One month later, the behavior of animals was assessed using the Open-field, Novel Object Location (NOL) test, Elevated-Plus Maze (EPM), and the Morris water maze (MWM). (**B**) Novel Object Location Test. The percentage of time exploring the new object location *versus* the total time was evaluated (Two-Way ANOVA with Tukey's post-hoc test, n=12 WT

Figure 7 continued on next page

Figure 7 continued

Scr shRNA, 14 WT *Dkk3* shRNA, 17 J20 Scr shRNA, 16 J20 *Dkk3* shRNA). (**C– E**) Morris Water Maze. (**C**) Representative traces for the MWM Trials 1 and 6 are shown. Graph on the right shows the escape latency. Two-way ANOVA with repeated measures showed a significant effect over trials (animal group $F_{(3,55)} = 16.97$, p-value <0.0001; trial $F_{(5,259)} = 42.94$, p-value = 0.457; animal group and trial interaction $F_{(15,275)} = 2.753$, p-value = 0.0006). For all analyses (n=12 WT Scr shRNA, 14 WT *Dkk3* shRNA, 17 J20 Scr shRNA, 16 J20 *Dkk3* shRNA). Graph show comparison between groups (Two-way ANOVA followed by Tukey's multiple comparisons). (**D, E**) Representative traces for the (**D**) Early and (**E**) Late probes. Graphs on the right show the time (s) to first reach the target location (Kruskal-Wallis followed by Dunns' multiple comparisons) and the distance (cm) traveled in the target quadrant (Two-way ANOVA followed by Tukey's post-hoc test for the early trial or Kruskal-Wallis followed by Dunns' multiple comparisons).

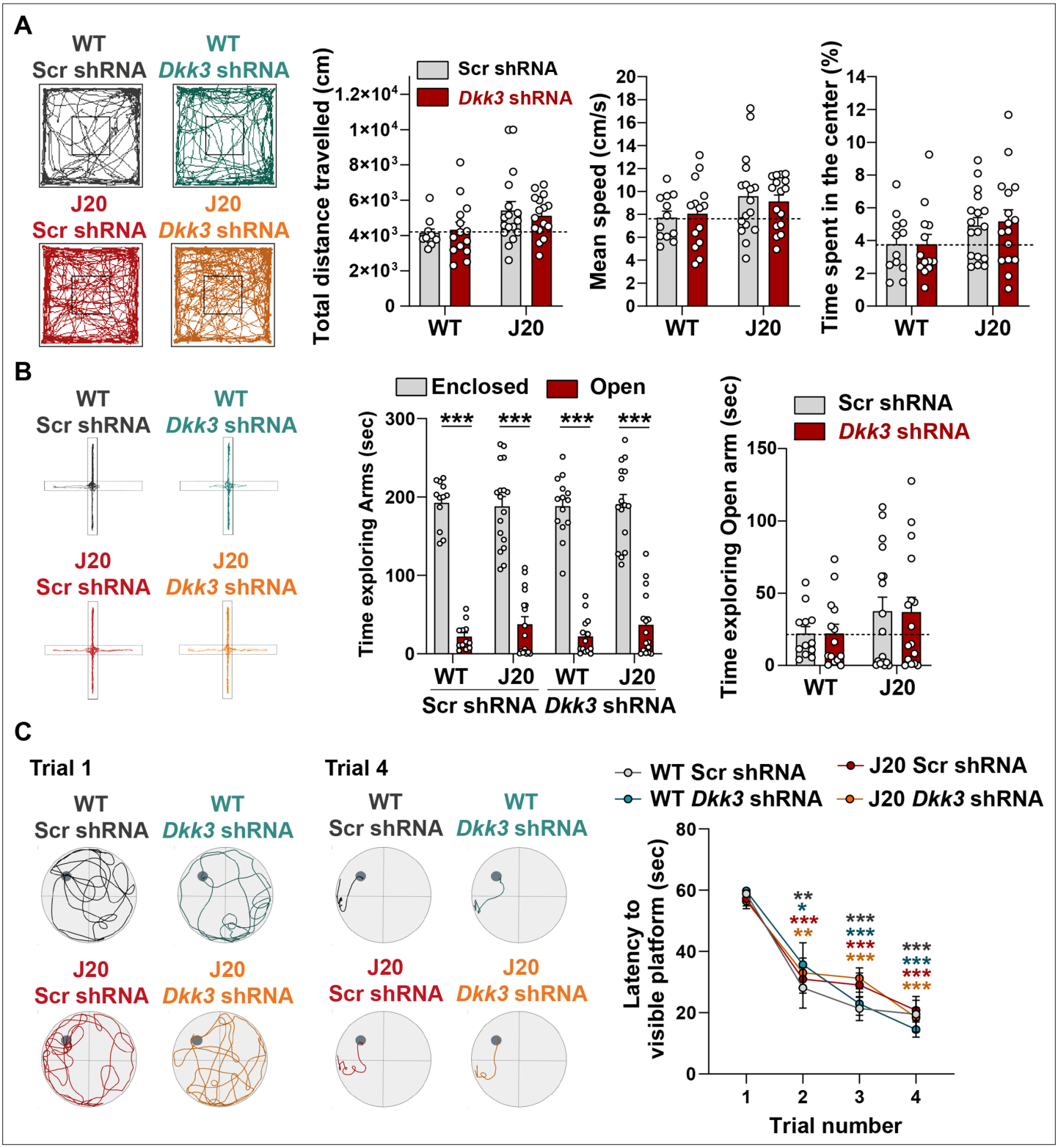

Figure 7—figure supplement 1. In vivo DKK3 loss-of-function does not affect locomotion or anxiety. (**A**) Open-field task. Representative traces of the open-field. Graphs show the total distance traveled in the open-filed (cm, left, Kruskal-Wallis test), mean speed (cm/s, middle, Two-way ANOVA) and the time spent in the center relative to the total time (%, right, Kruskal-Wallis test). (**B**) Elevated plus-maze (EPM). Representative traces of the EPM. Left graph shows the total time exploring arms (s, Two-way ANOVA followed by Tukey's multiple comparison test). Right graph displays the time spent in the open arms (s, Kruskal-Wallis test). (**C**) Morris Water Maze (MWM). Representative traces for Trials 1 and 4 in the training phase of the visible platform version of the MWM. The time (s) to reach the hidden platform was measured and compared over trials. No differences were observed between groups. (Two-Way ANOVA followed by Tukey's post-hoc test).